Journal of the Korean Physical Society, Vol. 67, No. 12, December 2015, pp. L2020∼L2025 Letters

First-principles Study on the Adsorption Properties of Phenylalanine on Carbon Graphitic Structures

Seoung-Hun Kang, Dae-Gyeon Kwon,* Sora Park† and Young-Kyun Kwon‡
Department of Physics and Research Institute for Basic Sciences, Kyung Hee University, Seoul 02447, Korea

(Received 16 November 2015, in final form 25 November 2015)

Using *ab-initio* density functional theory, we investigate the binding properties of phenylalanine, an amino acid, on graphitic carbon structures, such as graphene, nanotubes, and their modified structures. We focus especially on the effect of the adsorbate on the geometrical and the electronic structures of the absorbents. The phenylalanine molecule is found to bind weakly on pristine graphitic structures with a binding energy of $40-70$ meV and not to change the electronic configuration of the graphitic structures, implying that the phenylalanine molecule may not be detected on pristine graphitic structures. On the other hand, the phenylalanine molecule exhibits a substantial increase in its binding energy up to ∼2.60 eV on the magnesium-decorated boron-doped graphitic structures. We discover that the Fermi level of the system, which was shifted below the Dirac point of the graphitic structures due to *p*-doping by boron substitution, can be completely restored to the Dirac point because of the amino acid adsorption. This behavior implies that such modified structures can be utilized to detect phenylalanine molecules.

PACS numbers: 68.43.Bc, 61.46.-w, 73.22.-f, 87.85.fk
Keywords: Carbon graphitic structures, Phenylalanine, Adsorption property, Density functional theory
DOI: 10.3938/jkps.67.2020

I. INTRODUCTION

Carbon graphitic structures, such as graphene and carbon nanotubes (CNTs), have drawn diverse interests in multiple disciplines due to their unique physical and chemical properties [1–3]. With an expectation that they would replace silicon-based electronics in the near future, various carbon-based devices, which exhibits intriguing and unique characteristics, have been proposed [4–23]. Furthermore, some of these devices have been developed as sensors to detect various gases, chemicals, and biomolecules [24–36]. Compared to other existing sensors, these carbon-based sensors exhibit superior characteristics, such as their being compact, lightweight, and power efficient. They are also inexpensive because they can be mass-produced on a wafer level.

Among various analytes that can be detected by using graphitic structured materials, we focused on phenylalanine (Phe), one of the essential amino acids for the human body. Phe is converted into tyrosine, another essential amino acid, to produce signaling molecules, such as dopamine, epi norepinephrine (noradrenaline), epinephrine (adrenaline), and the skin pigment melanin. In addition, a genetic disorder called phenylketonuria (PKU) is caused by a deficiency of Phe hydroxylase, an enzyme to metabolize Phe [37,38]. People with this disorder, who are known as phenylketonurics, can suffer by serious problems such as mental retardation, irreversible brain damage, and seizures if they are left untreated. Although PKU is inherited and by far incurable, an optimal treatment to maintain blood Phe levels may prevent the development of serious mental incapacity [39–42], enabling PKU patients to have normal lives.

For such an optimal treatment, the quantitative monitoring of blood Phe levels together with the regulation of Phe intake, is an indispensable procedure. Phe levels in the blood have usually been measured by using centrifugation, which is costly and requires much time for a data analysis. Therefore, high-performance (quick and inexpensive) sensors to detect blood Phe levels, which could potentially provide a beneficial alternative to the existing newborn screening equipment, are in demand. We considered carbon graphitic materials as suitable candidates. Here, we show our study on the effect of Phe adsorption on the electronic properties of graphene and carbon nanotubes and their functionalized structures where two carbon atoms are replaced by two boron atoms with a magnesium atom [43]. Our finding reveals that Phe adsorption may not be detectable when using the pristine graphitic materials because these materials show no noticeable changes in their electronic structures. Our re-

*Current address: LG Chem Research Park, Daejeon 34122, Korea
†Electronics and Telecommunications Research Institute (ETRI), Daejeon 34129, Korea
‡E-mail: ykkwon@khu.ac.kr;

sults shows, however, that the modified graphitic structures respond substantially to Phe adsorption; thus, they may be utilized for Phe sensors.

II. COMPUTATIONAL DETAILS

To investigate the adsorption properties of Phe on carbon graphitic structures, we performed first-principles calculations using density functional theory (DFT) [44, 45]. An atomic orbitals basis with a double-ζ polarization was used to expand the electronic wave functions. We used the Ceperley-Alder exchange-correlation functional [46] in the local density approximation (LDA) as implemented in the SIESTA code [47]. Norm-conserving Troullier-Martins pseudopotentials [48] in the Kleinman-Bylander factorized form [49] were used to describe the behaviors of the valence electrons. We determined the potential and the charge density on a real-space grid with a mesh cutoff energy of 210 Ry, with which the total energy converged within 2 meV/atom. Using the conjugated gradient method [50], we allowed all atomic configurations to be relaxed without any symmetry constraints until none of the residual Hellmann-Feynman forces acting on any atom exceeded 10^{-3} Ry/$a_{\rm B}$, where $a_{\rm B}$ is the Bohr radius. To probe the possibility of magnetic ordering in the nanostructures, we used the local spin density approximation (LSDA) as a systematic way to estimate the net magnetic moments and the amount of exchange splitting in the systems.

To avoid the molecular interactions of the Phe molecule with those in neighboring unit cells, we arranged a 2D single layer of graphene in a hexagonal lattice with a lattice constant of 12.38 Å corresponding to a 5×5 supercell. Similarly, we prepared a 1D (8,0) or (5,5) nanotube with a lattice constant of 17.04 or 17.22 Å along its axial axis, including four or seven primitive unit cells, respectively. To suppress an interlayer or an intertube interaction, we also considered a large interlayer or an intertube distance of $\gtrsim 15$ Å.

In order to represent the Bloch wave functions adequately for the momentum space integration, we sampled the rather short Brillouin zone of these 2D and 1D structures with $3 \times 3 \times 1$ and $1 \times 1 \times 3$ k-point grids, respectively. For convergence test, the electronic structures of a few selected structures were calculated in a twice as dense k-point grid, and no significant difference was found. An isolated Phe molecule was described with one k-point at the Γ point in a cubic supercell with a length of 20 Å. A Mulliken population analysis was used to estimate the charge transfer between the adsorbate and the adsorbent within a single-ζ basis. The binding energy, E_b, of Phe on a host material is defined by

$$E_b = E(\text{Phe}) + E(\text{host}) - E(\text{Phe on host}),$$

where E(A) is the total energy of a system A.

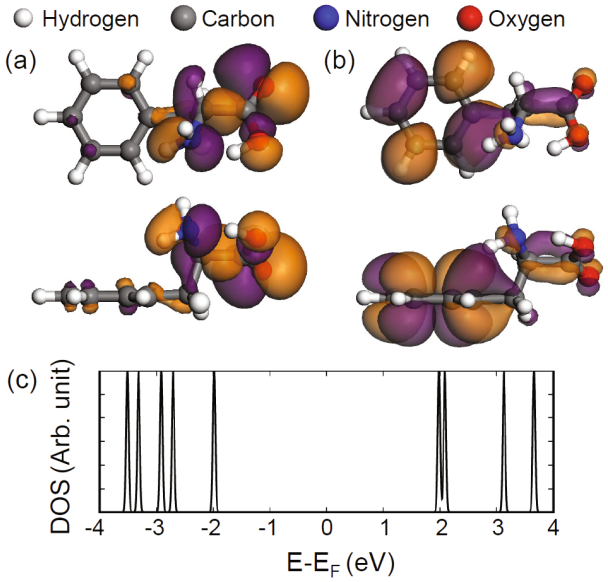

Fig. 1. (Color online) Two selected orbitals corresponding to the (a) HOMO and the (b) LUMO levels overlaid on the atomic structure (top and side views) of Phe. Different elements are depicted by different colors, as given in the legend. (c) Density of states of Phe showing a large HOMO-LUMO energy gap of 3.95 eV. The middle point between the HOMO and the LUMO levels was chosen to be the Fermi level and was set to zero.

III. RESULTS AND DISCUSSION

Before studying the adsorption property of Phe on a host carbon material, we first investigated the structural and the electronic properties of Phe itself, which is an α-amino acid with a chemical formula of $C_6H_5CH_2CH(NH_2)COOH$. A Phe molecule is composed of amine (–NH_2) and carboxyl acid (–COOH) groups along with a benzyl ($C_6H_5CH_2$–) side chain featuring a benzene ring attached to a methanediyl (–CH_2–) group, as shown in Fig. S1 in the Supporting Information. Figures 1(a) and (b) display the wave functions of the highest occupied molecular orbital (HOMO) and the lowest unoccupied molecular orbital (LUMO), respectively, overlaid on its equilibrium structure. The HOMO is dominant at the amine and the carboxyl acid groups, as shown in Fig. 1(a), while the LUMO is distributed mostly over the benzene ring, as displayed in Fig. 1(b). The HOMO-LUMO energy gap was found to be 3.95 eV from its density of states (DOS) shown in Fig. 1(c).

To inspect whether graphitic carbon materials can be used to detect Phe molecules, we explored the adsorption property of the Phe molecule on several graphitic carbon structures, such as graphene and (8,0) and (5,5) CNTs. We obtained the equilibrium configuration for each Phe-adsorbed host material by performing geometrical optimization with a variety of different initial configurations determined by using different molecular orientations and adsorption sites. For some selected configurations of

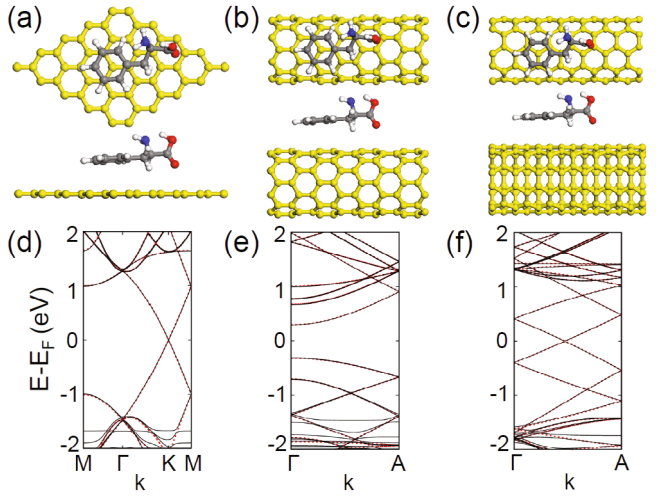

Fig. 2. (Color online) The optimized structures (top and side views) of Phe adsorbed on (a) graphene and on (b) $(8,0)$, and (c) $(5,5)$ carbon nanotubes, and (d–f) their corresponding band structures. For comparison, the host-only band structures are underlined with red dashed lines. For the respective elements, the same color scheme as that in Fig. 1, was used except for the host materials which are yellow-colored for distinction.

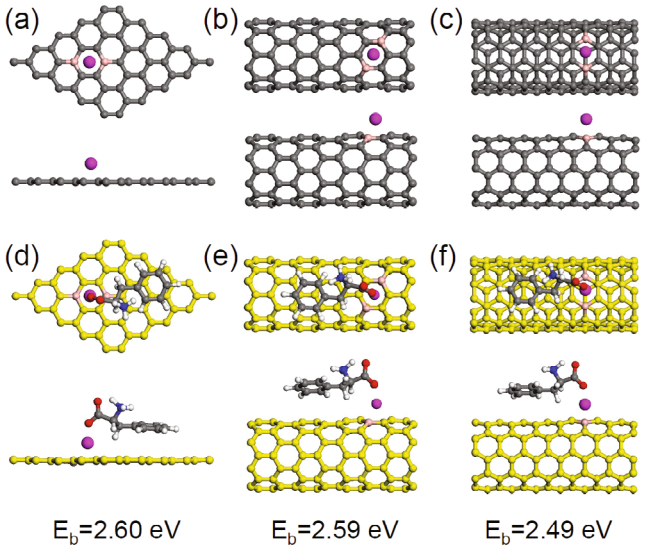

Fig. 3. (Color online) Equilibrium configurations of Mg-B_2-functionalized (a) graphene and (b) (10,0) and (c) (5,5) CNTs in top (upper) and side (bottom) views. (d–f) Equilibrium configurations of Phe-adsorbed on the corresponding structures given in (a–c), respectively. The calculated binding energies of the Phe molecule are given at the bottom.

Phe-adsorbed graphene, see Fig. S2 in the Supporting Information. Among these configurations are the most stable configurations shown in Figs. 2(a–c). In these equilibrium configurations, clearly, the Phe molecule tends to align its benzene ring over the graphitic structures similarly to "AB" stacking in graphite. Moreover, its double-bonded oxygen atom in the carboxyl acid (–COOH) group appears to face toward the graphene surface while its amine ($-NH_2$) group moves away from it, resulting in a structural deformation of the Phe molecule. The binding energy of a Phe molecule was numerically found to be $E_b \approx 0.66$, 0.44, and 0.41 eV on graphene and (8,0), and (5,5) CNTs, respectively, which are quite small. Our calculation also shows that the Phe molecule can diffuse on these graphitic materials with a low diffusion barrier of $\lesssim 20$ meV as long as the benzene ring keeps its orientation parallel to the graphene sheet.

Figures 2(d–f) show the corresponding electronic band structures, which are drawn with black solid lines, underneath which the host-material-only band structures are plotted with red dashed lines for comparison. Obviously, the Phe adsorption does not modify the electronic structures of any pristine graphitic carbon materials, except for a few flat bands around 1.8 eV below the Fermi level, which originate from the Phe HOMO levels. This observation, unfortunately, indicates that pristine graphitic carbon materials may not be used to detect Phe molecules. We also checked the effect of an external electric field (E-field), which can be easily applied through gating in the devices. No effect of E-field on electronic properties of the pristine graphitic carbon materials was found, as shown in Figs. S3 and S4 in the Supporting Information.

In order to utilize a graphitic material as a Phe sensor, clearly, one should enhance the reactivity of the host materials toward the adsorbate. To attain this, we considered alkaline-earth metal decoration on boron-doped graphitic structures, which were used for hydrogen binding enhancement [43]. Boron substitution makes the graphitic structures p-doped and plays the role as an acceptor to adsorb metal atoms. The two substituted boron atoms occupy the two farthest vertices in a hexagon, and the Mg atom is located in-between them and above the center of the hexagon, as shown in Figs. 3 (a–c).

We considered several different orientations of the Phe molecules adsorbed on various Mg-B_2-functionalized graphitic structures, such as graphene and both $(8,0)$ and $(5,5)$ CNTs, to find the most stable binding configuration for each case. We found that the Mg atom tended to interact with the double-bonded oxygen atom in the carboxyl acid (–COOH) group of the Phe molecule. Through this interaction, we found an intriguing "bond exchange" process, in which the C=O double bond became a C–O^- bond that binded to the Mg atom, strengthening the Phe binding, while the C–O–H bond lost the hydrogen atom, becoming a C=O bond. The removed hydrogen atom was observed to encounter the amine ($-NH_2$) group to form $-NH_3^+$. The most stable structures of the three cases are displayed in Figs. 3 (d–f). The binding energies of a Phe molecule on these functionalized structures were calculated to be $2.5 \sim 2.6$ eV, which are about 30 times stronger than the values for

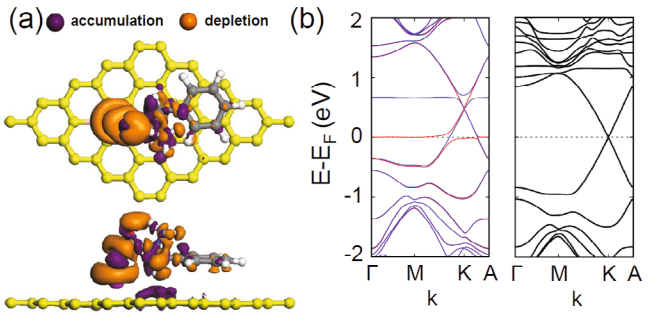

Fig. 4. (Color online) (a) Isosurface plot in top and side views of the charge density difference in the optimized structure of Phe-adsorbed Mg-B_2-functionalized graphene. For the respective elements, the same color scheme as that in Fig. 1, was used except for graphene being yellow-colored for distinction. The isovalue is ± 0.001 e Å^{-3}. (b) Band structures along the high-symmetry lines of Mg-B_2-functionalized graphene with (right) and without (left) the Phe adsorption. In the left graph, the red and the blue curves represent spin majority and minority bands, respectively.

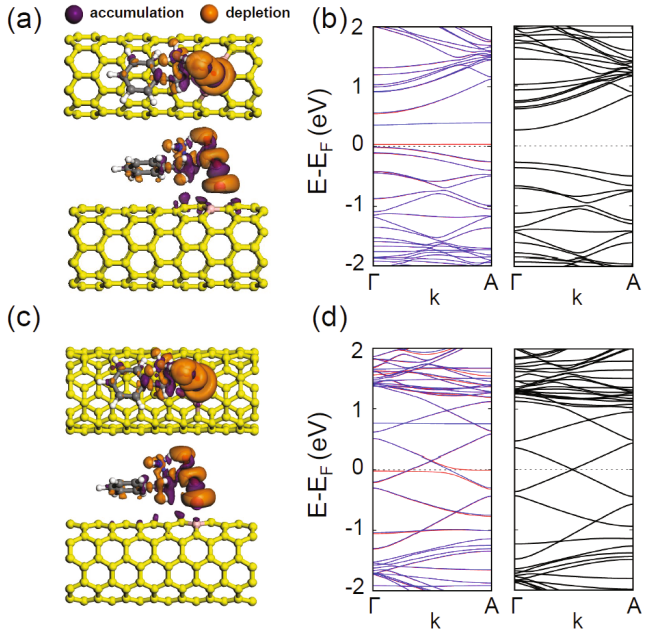

Fig. 5. (Color online) (a) Equilibrium structure with charge density difference of Phe-adsorbed (a) $(8,0)$, and (c) $(5,5)$ CNTs functionalized with Mg-B_2. (b) and (d) Their respective band structures and host-only band structures. For the respective elements, the same color scheme as that in Fig. 1, was used except for the CNTs being yellow-colored for distinction. The isovalue of ± 0.001 e/Å was used for charge density difference in (a) and (c). In the band structure, the spin majority and minority bands are depicted with red and blue lines, respectively.

their pristine counterparts.

To explore the electronic structure modification, we calculated the charge density difference of Phe-adsorbed Mg-B_2-functionalized graphene. As displayed in Fig. 4, electrons are accumulated on the side of the Mg-B_2-functionalized graphene while being depleted on the Phe side. In addition, a charge redistribution in the Phe molecule was found to occur because of the reconstruction of the Phe structure caused by the bond exchange mechanism, as mention above. Figure 4(b) shows the electronic band structures of the Mg-B_2-functionalized graphene with (right) and without (left) the adsorbed Phe molecule. The left band structure can be interpreted as follows: Two boron atoms substitute for two carbon atoms, hole-doping graphene and shifting its Fermi level down. As a result, the band crossing point or Dirac point at K is located above the Fermi level. The added magnesium atom, which has two valence electrons, plays a role as a donor, providing only one valence electron to the B_2-doped graphene and shifting the Fermi level halfway up; thus, its flat or localized valence states become split: one state occupied and one empty being spin-polarized. Surprisingly, we found that Phe adsorption not only restores its Fermi level exactly to that of the pristine graphene but also changes the Mg spin-polarized states to nonmagnetic degenerate states, as shown in the right graph in Fig. 4(b). We can deduce from the charge redistribution on the adsorbed Phe molecule shown in Fig. 4(a) that the Phe molecule takes an electron from the Mg atom and gives it to the graphene. As a result, the emptied Mg levels are pushed away from the Fermi level, as seen in the right graph of Fig. 4(b). Note that such an exact restoration of the Fermi level is due to the one-to-one matching of the Mg-B_2 doping rate and the Phe concentrations. Lower concentration of Phe adsorption may not restore the Fermi level completely while a higher concentration may not be able to shift the Fermi level further up because Phe adsorption on a pristine graphene surface does not change anything, as discussed above. This observation implies that Mg-B_2-functionalized graphene may be used to detect the existence of Phe molecules. We also checked the effect of an external E-field and found that the electronic properties were robust for the external E-field. (See Fig. S5 in the Supporting Information.)

We also explored the electronic structure modification of the Mg-B_2-functionalized (8,0) and (5,5) CNTs due to Phe molecule adsorption. As discussed above, Phe binding is enhanced through a bond exchange mechanism. As on Mg-B_2-functionalized graphene, small charge accumulations were observed on both functionalized (8,0) and (5,5) CNTs while a charge depletion and redistribution were observed on the Phe molecule, as shown in Figs. 5(a) and (c). Figures 5(b) and (d) show the electronic structures of the Mg-B_2-functionalized (8,0) and (5,5) CNTs without and with the adsorbed Phe molecule, respectively. Similar to the Mg-B_2-functionalized graphene shown in Fig. 4(b), the Mg-B_2-functionalized CNTs becomes hole-doped and spin-polarized mainly by Mg valence states. In both cases, Phe adsorption brings back the Fermi levels of their pristine counterparts. These results indicate that such func-

tionalized graphitic materials can be utilized as a sensing platform to detect Phe molecules for PKU treatment.

IV. CONCLUSION

In summary, we investigated the adsorption properties of phenylalanine on pristine and Mg-B_2-functionalized graphitic carbon materials, such as graphene and nanotubes using density functional theory calculations. We found that a Phe molecule binds quite weakly on the pristine carbon structures; thus, these carbon structures undergo almost no modification. However, Mg-B_2 functionalization interacts strongly with a Phe molecule to initiate the so-called bond exchange mechanism to enhance the binding by about 30 times. The Fermi levels of the Mg-B_2 hole-doped graphitic structures were found to be shifted downward, but Phe-adsorption restored it to where it had been in the pristine counterpart. This study may shed light on the development of a simple scheme for detecting amino acids.

ACKNOWLEDGMENTS

This work was supported by a grant (KHU-20100658) from Kyung Hee University. Some portion of our computational work was done using the resources of the Korea Institute of Science and Technology Information (KISTI) Supercomputing Center (KSC-2015-C3-048).

REFERENCES

[1] J. W. Mintmire, B. I. Dunlap and C. T. White, Phys. Rev. Lett. **68**, 631 (1992).
[2] C. Dekker, Phys. Today **52**, 22 (1999).
[3] A. H. Castro Neto, F. Guinea, N. M. R. Peres, K. S. Novoselov and A. K. Geim, Rev. Mod. Phys. **81**, 109 (2009).
[4] Y.-K. Kwon, D. Tománek, and S. Iijima, Phys. Rev. Lett. **82**, 1470 (1999).
[5] R. Martel, V. Derycke, C. Lavoie, J. Appenzeller, K. Chan, J. Tersoff and P. Avouris, Phys. Rev. Lett. **87**, 256805 (2001).
[6] A. Bachtold, P. Hadley, T. Nakanishi and C. Dekker, Science **294**, 1317 (2001).
[7] S. Heinze, J. Tersoff, R. Martel, V. Derycke, J. Appenzeller and P. Avouris, Phys. Rev. Lett. **89**, 106801 (2002).
[8] A. Javey, J. Guo, Q. Wang, M. Lundstrom and H. Dai, Nature **424**, 654 (2003).
[9] M. Lee, J. Im, B. Y. Lee, S. Myung, J. Kang, L. Huang, Y.-K. Kwon and S. Hong, Nat. Nanotechnol. **1**, 66 (2006).
[10] E. Castro, K. Novoselov, S. Morozov, N. Peres, J. dos Santos, J. Nilsson, F. Guinea, A. Geim and A. Neto, Phys. Rev. Lett. **99**, 216802 (2007).
[11] Z. Chen, Y.-M. Lin, M. J. Rooks and P. Avouris, Physica E **40**, 228 (2007).
[12] A. Rycerz, J. Tworzydlo and C. W. J. Beenakker, Nat. Phys. **3**, 172 (2007).
[13] A. F. Young and P. Kim, Nat. Phys. **5**, 13 (2008).
[14] M. Lee, K. Y. Baik, M. Noah, Y.-K. Kwon, J.-O. Lee and S. Hong, Lab Chip **9**, 2267 (2009).
[15] M. Lee, M. Noah, J. Park, M.-J. Seong, Y.-K. Kwon and S. Hong, Small **5**, 1642 (2009).
[16] J. Wu, M. Agrawal, H. A. Becerril, Z. Bao, Z. Liu, Y. Chen and P. Peumans, ACS Nano **4**, 43 (2010).
[17] S. Myung, S. Woo, J. Im, H. Lee, Y.-S. Min, Y.-K. Kwon and S. Hong, Nanotechnology **21**, 345301 (2010).
[18] F. Xia, D. B. Farmer, Y.-M. Lin and P. Avouris, Nano Lett. **10**, 715 (2010).
[19] K. S. Novoselov, V. I. Fal'ko, L. Colombo, P. R. Gellert, M. G. Schwab and K. Kim, Nature **490**, 192 (2012).
[20] S. Dröscher, C. Barraud, K. Watanabe, T. Taniguchi, T. Ihn and K. Ensslin, New J. Phys. **14**, 103007 (2012).
[21] Y. L. Kim, H. Y. Jung, S. Park, B. Li, F. Liu, J. Hao, Y.-K. Kwon, Y. J. Jung and S. Kar, Nat. Photonics **8**, 239 (2014).
[22] L. Ju, Z. Shi, N. Nair, Y. Lv, C. Jin, J. Velasco Jr, C. Ojeda-Aristizabal, H. A. Bechtel, M. C. Martin, A. Zettl, J. Analytis and F. Wang, Nature **520**, 650 (2015).
[23] S.-H. Kang, G. Kim and Y.-K. Kwon, Phys. Chem. Chem. Phys. **17**, 5072 (2015).
[24] S. Sotiropoulou and N. A. Chaniotakis, Anal. Bioanal. Chem. **375**, 103 (2003).
[25] A. Star, K. Bradley, J.-C. P. Gabriel and G. Grüner, Prepr. Pap.-Am. Chem. Soc., Div. Fuel Chem. **49**, 887 (2004).
[26] L. Piao, Q. Liu, Y. Li and C. Wang, J. Phys. Chem. C **112**, 2857 (2008).
[27] H. Song, Y. Lee, T. Jiang, a. G. Kussow, M. Lee, S. Hong, Y.-K. Kwon and H. Choi, J. Phys. Chem. C **112**, 629 (2008).
[28] C.-H. Lu, H.-H. Yang, C.-L. Zhu, X. Chen and G.-N. Chen, Angew. Chem. **121**, 4879 (2009).
[29] M. Ganji, Diam. Relat. Mater. **18**, 662 (2009).
[30] C. Rajesh, C. Majumder, H. Mizuseki and Y. Kawazoe, J. Chem. Phys. **130**, 124911 (2009).
[31] L. Piao, Q. Liu, Y. Li and C. Wang, J. Nanosci. Nanotechnol. **9**, 1394 (2009).
[32] Z. Wang, M. Gerstein and M. Snyder, Nat. Rev. Genet. **10**, 57 (2009).
[33] M. Pumera, A. Ambrosi, A. Bonanni, E. L. K. Chng and H. L. Poh, Trac-Trends Anal. Chem. **29**, 954 (2010).
[34] B. Y. Lee, M. G. Sung, J. Lee, K. Y. Baik, Y.-K. Kwon, M.-S. Lee and S. Hong, ACS Nano **5**, 4373 (2011).
[35] H.-J. Lee, G. Kim and Y.-K. Kwon, Chem. Phys. Lett. **580**, 57 (2013).
[36] H. Y. Jung, Y. L. Kim, S. Park, A. Datar, H.-J. Lee, J. Huang, S. Somu, A. Busnaina, Y. J. Jung and Y.-K. Kwon, Analyst **138**, 7206 (2013).
[37] W. R. Centerwall, S. A. Centerwall, V. Armon and L. B. Mann, J. Pediatr. **59**, 102 (1961).
[38] R. Williams, A. Cyril, D. S. Mamotte and J. R. Burnett, Clin. Biochem. Rev. **29**, 31 (2008).
[39] B. K. Burton, D. K. Grange, A. Milanowski, G. Vockley, F. Feillet, E. A. Crombez, V. Abadie, C. O. Harding, S. Cederbaum, D. Dobbelaere, A. Smith and A. Doren-

baum, J. Inherit. Metab. Dis. **30**, 700 (2007).
[40] R. Guthrie and A. Susi, Pediatr. **32**, 338 (2007).
[41] C. R. Scriver, J. Clin Invest. **101**, 2613 (1998).
[42] H. Bickel, J. Gerrard and E. M. Hickmans, Acta Paediatr. **43**, 64 (1954).
[43] G. Kim, S.-H. Jhi, S. Lim and N. Park, Phys. Rev. B **79**, 155437 (2009).
[44] P. Hohenberg and W. Kohn, Phys. Rev. **136**, B864 (1964).
[45] W. Kohn and L. J. Sham, Phys. Rev. **140**, A1133 (1965).
[46] D. M. Ceperley and B. J. Alder, Phys. Rev. Lett. **45**, 566 (1980).
[47] J. M. Soler, E. Artacho, J. D. Gale, A. García, J. Junquera, P. Ordejón and D. Sánchez-Portal, J. Phys.: Condens. Matter **14**, 2745 (2002).
[48] N. Troullier and J. L. Martins, Phys. Rev. B **43**, 1993 (1991).
[49] L. Kleinman and D. M. Bylander, Phys. Rev. Lett. **48**, 1425 (1982).
[50] M. R. Hestenes and E. Stiefel, J. Res. Natl. Bur. Stand. **49**, 409 (1952).